Research Paper
Computational Methods for Differential Equations
http://cmde.tabrizu.ac.ir
Vol. *, No. *, *, pp. 1-17
DOI:10.22034/cmde.2024.61873.2695

Analyzing MHD boundary layer flow of Rivlin Ericksen fluid over a stretching sheet by applying Taylor Wavelet Approach

Prithvi Suresh, Vidya Shree Ramareddy, and Patil Mallikarjun Basavaraj*

Department of Studies and Research in Mathematics, Tumkur University, Tumkur-572103, Karnataka, India.

Abstract

In the current paper, we newly established the Taylor wavelet operational matrix method to study Revlin Ericksen fluid flowing over the stretching sheet in the context of magnetic field. Taylor wavelet operational matrix method is newly devised method for transforming the non linear differential equations to nonlinear algebraic equations. This computation is flexible and facile due to the generation of integral matrices. From these integral matrices unresolved Taylor wavelet coefficients are determined with the help of solvers. Thus solution to the given Revlin Ericksen fluid flow is achieved. This analysis examines MHD Rivlin-Ericksen fluid flowing in the steady state caused by stretching a sheet while accounting for inverse Darcy model. The aforementioned computational method is for seeking solution to ordinary differential equations. Firstly, the momentum equation is changed to ordinary differential equation by employing the similarity transformation then Taylor wavelet method has to be implemented for further analysis. The effect of viscoelastic parameter, inverse Darcy number, magnetic parameter and inclination angle on axial and transverse velocity are taken into consideration for study analysis. Engineering application tool Local skinfriction coefficient variation has been assessed for different parameters and estimated local skin friction coefficient is compared with bvp4c demonstrating compatibility of Taylor wavelet approach.

Keywords. Operational integration matrix, Rivlin erickson fluid, Taylor wavelet, Stretching sheet,Collocation method.
2010 Mathematics Subject Classification. 65L05, 34K06, 34K28.

1. Introduction

The industrial applications of making plastic sheets from synthetic materials are expanding on a daily basis, necessitating the description of the intrinsic phenomena involved. Numerical output for momentum equation obtained through wavelet method has been bench marked with the exact solution as the validation procedure. Theoretical model was first developed for a particular fluid known as Revlin- erickson fluid by Rivlin-erickson [19] and the elasticity of the material has been explored with the help of single-valued energy strain function. Effect of Rivlin erickson fluid flow over the boundary has been evaluated by Siddappa and Khapate [26] which is an extension of Crane's [3] work. The importance of studying the non-newtonian fluid is that it has wide range of applications such as communication devices, industrial applications, agricultural areas and biomedical devices.

There are several non-newtonial fluids such as williamson fluid, casson fluid etc among them Rivlin Erickson fluid is one of such fluids which has been used in tyres, ceramic materials, foams and filtration process etc. Sharma and Kumar [21] has shown the Stabilizing impact of the rotation on Rivlin-Erickson fluid flow. Laplace transform method has been implemented to obtain the exact solution of second-grade Rivlin-Erickson fluid flow for rayleigh's problem by Jordan and Puri [8] and has observed the steady state configuration due to discontinuity arising in the beginning. With the help of dispersion equation stability analysis has made for viscoelastic fluid by Kumar and Singh [12]. Shukla and Awasthi [24] explored Wave number and Perturbation growth variation and visualized in the form of graphs. They have assessed that interface becomes unstable when thickness grows through Newton Raphson method.

Received: 29 May 2024 ; Accepted: 20 January 2025.
* Corresponding author. Email: mbp1007@yahoo.com .

Pradeep *et al.* [11] have inferred that there is both stabilizing and destabilizing effect in the presence of magnetic field and stabilizing effect on rotating the viscoelastic fluid. Kareem *et al.* [9] solved the energy balance and momentum equations by finite difference method and inferred that lower dissipation rate minimizes the entropy production. Convection of oscillatory and non oscillatory systems for various parameters such as Kinematic number, Vadasz number and Lewis number have been studied by Chand and Rana [2]. Slemrod [27] has expressed Polymeric fluids as a function of Rivlin-Erickson tensor. Top-heavy and bottom-heavy configuration has been explained by sharma *et al.* [22] and they observed Kelvin-helmoltz instability in the presence of surface tension for Rivlin-Erickson fluid embedded with porous media.

Gupta *et al.* [7] has investigated suspended particles and hall current impact of elastico-viscous fluid and analyzed the stability by linearizing the hydromagnetic perturbed equations. considered steady mass flux over a semi-infinite plate to study the impact of thermal diffusion and diffusion-thermo for Rivlin-Erickson fluid. Reddy *et al.* [18]. Dharamendra *et al.* [5] has comparitively studied the stability of viscous fluid-viscous fluid interface and Rivlin-Erickson fluid-viscous fluid interface concluding that viscous fluid-viscous fluid interface is less stable compared to Rivlin-Erickson fluid-viscous fluid interface. Moatimid and Sayed [15] plotted stability plots for various parameters and investigated stability for two Rivlin-Erickson fluid having cylindrical interface. Prescribed heat flux and prescribed temperature cases are analyzed by making use of Kummer's function and hence the closed form of analytical solution is obtained by Vishalakshi *et al.* [32]. Akbar *et.al* [1] analysed the effect of magnetic field fow the flow of eyring powell fluid and found that increased eyring powell parameter and magnetic field parameter decreases the fluid velocity.

Time signals are monitored and evaluated due to its applications in various systems. For stationary time signals Joseph Fourier in 1807 developed a transform known as Fourier Transform. Alfred Haar in 1909 found out the transform for non-stationary signals and Haar was the one who first time called this transform as wavelet transform. Keshavarz *et al* [10] pioneeered the Taylor wavelet generation for solving initial and boundary valued problems. Error analysis has been done for Benjamin-Bona-Mahony partial differential equation by Shiralashetti and Hanaji [23]. Ratish and Mehra [17] used Taylor wavelet Galerkin scheme to solve Burger's equation by separating the diffusion and advection terms. Orthonormality of Taylor wavelet has been considered by Sevin [6] to obtain solution for the Lane-Emden equations. Riemann-Liouville fractional integral equation has been explored by Toan *et al* [28].

A substantial research work has been carried out in wavelets for obtaining solution in the field of Fluid dynamics. The undershoots and overshoots of a viscous fluid in the presence of magnetic field has been studied with the help of Bernoulli collocation method by Vivek and Kumar [33]. Vidyashree *et al* [29] employed Legendre wavelet operational matrix method to explore the impact of magnetic and pressure gradient parameter on the boundary layer thickness for the fluid flowing over a stretching sheet. Equations arising in fluid dynamics and astrophysics such as Emden-Fowler type equations has been tackled by Fibonacci wavelet method by Manohara and Kumbinarasaiah [14]. The effect of casson parameter, Grashof and Biot number on entropy generation for the casson fluid flowing in a vertical channel has been discussed by Vidyashree *et al* [16]. Some other research work are also been carried out in the fluid dynamics field recently [4, 20, 25, 30, 31].

The current investigation aims to enhance Vishalakshi *et al.* [32] work by incorporating the newly constructed Taylor wavelet operational matrix. The innovative aspect of this work is application of Taylor wavelet approach to solve non linear momentum equation of Revlin Erickson fluid flowing past the stretching sheet. Skin friction and Nusselt number were examined. The impact of various physical characteristics is investigated via graphical representation. Various works has been carried out related to Revlin Erickson fluid flow none of them has been solved using wavelet method as per the literature survey this makes the current study more significant and interesting.

2. Mathematical Model and Formulation

This work examines the consistent two-dimensional MHD flow of an electrically operating, incompressible Revlin-Ericksen fluid over a porous stretching/shrinking sheet with the inverse Darcy model is depicted in the Figure 1. The flow is studied in the presence of inclined magnetic field. This extends the work of Siddappa and Hiremath [25].

Maxwell's equation for the flow [32]

$$\vec{J} = \mu_m \sigma(\vec{q} \times \vec{B}), \tag{2.1}$$

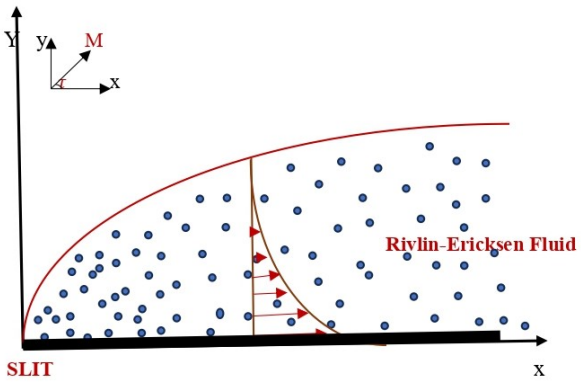

FIGURE 1. Rivlin Ericken fluid past a stretching sheet.

$$\nabla.\vec{B} = 0, \tag{2.2}$$

$$\nabla \times \vec{B} = \sigma \vec{E_{induced}}, \tag{2.3}$$

$$\nabla \times \vec{E_{induced}} = -\mu_m \frac{\partial \vec{B}}{\partial t}. \tag{2.4}$$

Porous media is injected in the fluid flow and a homogeneous inclined magnetic field of strength B_0 is applied. Lorentz force for electrically weak conducting fluid is $\mu_m \vec{J} \times \vec{B} sin^2\tau$ which results in

$$\mu_m \vec{J} \times \vec{B} sin^2\tau = -\mu^2 \sigma B_0^2 sin^2\tau u. \tag{2.5}$$

As per the above consideration the governing boundary layer equation [32] is

$$\frac{\partial u}{\partial x} + \frac{\partial u}{\partial y} = 0, \tag{2.6}$$

$$u\frac{\partial u}{\partial x} + v\frac{\partial u}{\partial y} = \nu\frac{\partial^2 u}{\partial y^2} + k_1\left[\left(u\frac{\partial u}{\partial x} + v\frac{\partial u}{\partial y}\right)_{yy} + 2\left(\frac{\partial u}{\partial x}\frac{\partial u}{\partial y}\right)_y\right] + \gamma\left(\left(\frac{\partial u}{\partial y}\right)^2\right)_x - \left(\frac{\sigma B_o^2 sin^2(\tau)}{\rho} + \frac{\mu}{\rho K}\right)u, \tag{2.7}$$

complementing boundary conditions [4]

$$v = 0, \quad u = ax, \quad \text{at} \quad y = 0, \tag{2.8}$$

$$u \to 0, \quad \frac{\partial u}{\partial y} \to 0, \quad \text{as} \quad y \to \infty, \tag{2.9}$$

similarity transformation to non dimensionalize the above equations

$$u = axf'(\eta), \quad v = -\sqrt{a\nu}f \quad \text{and} \quad \eta = \sqrt{\frac{a}{\nu}}y. \tag{2.10}$$

Substituting Eq. (2.10) in Eq. (2.7) we obtain the ordinary differential equation

$$f'^2 - ff'' - f''' - \beta(2f'f''' + 3f''^2 - ff'''') - 2\gamma f''^2 + (Msin^2(\tau) + Da^{-1})f' = 0, \tag{2.11}$$

corresponding boundary conditions reduces to

$$f(0)=0, \quad f'(0)=1, \quad f'(\infty)\to 0 \quad \text{and} \quad f''(\infty)\to 0, \tag{2.12}$$

where $M=\frac{\sigma {B_0}^2}{\rho a}$, $\beta=\frac{k_1 a}{\gamma}$ and $Da^{-1}=\frac{\mu}{\rho a K}$.

The local skin friction coefficient is $Cf_x=\frac{\tau_w}{\rho u_\infty^2}$ where τ_w is wall shear stress.

$$Re_x^{\frac{1}{2}} Cf_x=(1-3\beta)f''(0). \tag{2.13}$$

3. Taylor wavelet and its operational matrix

Definition 3.1 (Taylor wavelet [10])**.** Taylor wavelet function over the interval $[0,1)$ with v being the set of all natural numbers upto $V-1$ along with zero, $u=1$ to 2^{l-1} and $l\in Z^+$.

$$\xi_{u,v}(q)=\begin{cases} 2^{\frac{-1+l}{2}}\overline{\xi}_v(2^{-1+l}q+1-u), & \text{if } \ 2^{\frac{u-1}{2l-1}}\le q\le 2^{\frac{u}{2l-1}},\\ 0, & \text{otherwise.}\end{cases} \tag{3.1}$$

with $\overline{\xi}_v(q)=\frac{\xi_v(q)}{\sqrt{2n+1}}$, where $\xi_v(q)=q^v$

Approximating function: Expressing $F(q)$ in terms of Taylor wavelet basis:

$$F(q)\approx \sum_{u=1}^{\infty}\sum_{v=1}^{\infty} R_{u,v}\xi_{u,v}(q). \tag{3.2}$$

$$F(q)\approx \sum_{u=1}^{2^{l-1}}\sum_{v=0}^{V-1} R_{u,v}\xi_{u,v}(q)=R^T T_y(q). \tag{3.3}$$

where R and $T_y(q)$ are $2^{l-1}V\times 1$ matrices,

$$R=[R_{1,0}.....R_{1,V-1}\ R_{2,0}.....R_{2,V-1}....R_{2^{l-1},V-1}],$$

and

$$T_y(q)=[\xi_{1,0}....\xi_{1,V-1}\ \xi_{2,0}.... \xi_{2,D-1}.... \xi_{2^{l-1},V-1}].$$

For $V=10$ and $l=1$ Taylor wavelet basis fetched which are given as follows :

$$\xi_{1,0}(q)=1, \qquad \xi_{1,1}(q)=\sqrt{3}q,$$
$$\xi_{1,2}(q)=\sqrt{5}q^2, \qquad \xi_{1,3}(q)=\sqrt{7}q^3,$$
$$\xi_{1,4}(q)=3q^4, \qquad \xi_{1,5}(q)=\sqrt{11}q^5,$$
$$\xi_{1,6}(q)=\sqrt{13}q^6, \qquad \xi_{1,7}(q)=\sqrt{15}q^7,$$
$$\xi_{1,8}(q)=\sqrt{17}q^8, \qquad \xi_{1,9}(q)=\sqrt{19}q^9,$$

where $T_{y10}(q)=[\xi_{1,0}\ \ \xi_{1,1}\ \ \xi_{1,2}\ \ \xi_{1,3}\ \ \xi_{1,4}\ \ \xi_{1,5}\ \ \xi_{1,6}\ \ \xi_{1,7}\ \ \xi_{1,8}\ \ \xi_{1,9}]^T$.

Theorem 3.2. *If $F(q)$ is a bounded continuous function defined in $H^2[0,1)$ then the Taylor wavelet expansion of $F(q)$ converges to it*

Proof. Let F(q) be a continuous bounded real valued function defined on $[0,1)$ then the taylor coefficients of F(q) is given as

$$R_{u,v}=\int_0^1 F(q)\xi_{u,v}(q)dq,$$

$$R_{u,v}=\int_I F(q)\frac{2^{\frac{l-1}{2}}}{\sqrt{2u+1}}\xi_v(2^{l-1}q+1-u)dx, \quad \text{where} \quad I=[2^{\frac{u-1}{2l-1}}, 2^{\frac{u}{2l-1}}),$$

put $\quad 2^{l-1}q+1-u=z,$

$$R_{u,v} = \int_{-1}^{1} F\left(\frac{z+u-1}{2^{l-1}}\right) \frac{2^{\frac{l-1}{2}}}{\sqrt{2u+1}} \xi_v(z) 2^{1-l} dz,$$

$$R_{u,v} = \frac{2^{\frac{-l+1}{2}}}{\sqrt{2u+1}} \int_{-1}^{1} F\left(\frac{z+u-1}{2^{l-1}}\right) \xi_v(z) dz,$$

by gauss mean value theorem for integrals we have,

$$R_{u,v} = \frac{2^{\frac{-l+1}{2}}}{\sqrt{2u+1}} F\left(\frac{w+u-1}{2^{l-1}}\right) \int_{-1}^{1} \xi_v(z) dz, \quad \text{for some } w \in (-1,1),$$

put $\int_{-1}^{1} \xi_v(z) dz = g$,

$$|R_{u,v}| = \left|\frac{2^{\frac{-l+1}{2}}}{\sqrt{2u+1}}\right| \left|F\left(\frac{w+u-1}{2^{l-1}}\right)\right| g.$$

since F(q) is a bounded function hence $\sum_{u,v=0}^{\infty} R_{u,v}$ is absolutely convergent. Therefore the Taylor series expansion converges uniformly □

Theorem 3.3. *Consider $F(q) \in C^p[0,1)$ where $C^p[0,1)$ is p times continuously differentiable function and $\xi_{u,v}$ be Taylor wavelet sequence. Let $F(q) = \sum_{u=1}^{2^{k-1}} F_u(q)$ and $f_u(q) = L(\xi_{u,v})$ be the linear space spanned by $\xi_{u,v}$. If $R^T T_y(q)$ is best approximation from $f_u(q)$ to $F_u(q)$ then $R^T T_y(q)$ approximates with the following error bound.*

$$||F(q) - R^T T_y(q)|| \le K \sqrt{\left(\frac{\left(2^{\frac{u}{2l-1}} - 2^{\frac{u-1}{2l-1}}\right)^{2p+1}}{(2p+1)}\right)},$$

Proof. The Taylor expansion for the function $F_u(q)$ is

$$\overline{F_u(q)} = F_u(2^{\frac{u-1}{2l-1}}) + F'_u(2^{\frac{u-1}{2l-1}}) \frac{\left(x - 2^{\frac{u-1}{2l-1}}\right)}{1!} + ... + F_u^{p-1}(2^{\frac{u-1}{2l-1}}) \frac{\left(x - 2^{\frac{u-1}{2l-1}}\right)^{p-1}}{(p-1!)},$$

we know that

$$|F_u(q) - \overline{F_u(q)}| \le |F_u^p(q)| \frac{\left(x - 2^{\frac{u-1}{2l-1}}\right)^p}{(p!)}, \text{ where } q \in \left[2^{\frac{u-1}{2l-1}}, 2^{\frac{u}{2l-1}}\right), \tag{3.4}$$

$$||F_u(q) - R^T T_y(q)||^2 \le ||F_u(q) - \overline{F_u(q)}||^2,$$

$$\int_{2^{\frac{u-1}{2l-1}}}^{2^{\frac{u}{2l-1}}} |F_u(q) - \overline{F_u(q)}|^2 \le \int_{2^{\frac{u-1}{2l-1}}}^{2^{\frac{u}{2l-1}}} \left(|F_u^p(q)| \frac{\left(x - 2^{\frac{u-1}{2l-1}}\right)^p}{(p!)}\right)^2 dx, (fromeqn.(17))$$

$$= \left(\frac{F_u^p(q)}{p!}\right)^2 \left(\frac{\left(x - 2^{\frac{u-1}{2l-1}}\right)^{2p+1}}{(2p+1)}\right)\Bigg|_{2^{\frac{u-1}{2l-1}}}^{2^{\frac{u}{2l-1}}},$$

$$= \left(\frac{F_u^p(q)}{p!}\right)^2 \left(\frac{\left(2^{\frac{u}{2l-1}} - 2^{\frac{u-1}{2l-1}}\right)^{2p+1}}{(2p+1)}\right),$$

$$= K\left(\frac{\left(2^{\frac{u}{2l-1}} - 2^{\frac{u-1}{2l-1}}\right)^{2p+1}}{(2p+1)}\right), \tag{3.5}$$

where $K = \left(\frac{F_u^p(q)}{p!}\right)^2$. Now consider,

$$||F(q) - R^T T_y(q)||^2 \leq \sum_{2^l-1}^{u-1} ||F_u(q) - R^T T_y(q)||^2,$$

$$||F(q) - R^T T_y(q)||^2 \leq K^2\left(\frac{\left(2^{\frac{u}{2l-1}} - 2^{\frac{u-1}{2l-1}}\right)^{2p+1}}{(2p+1)}\right),$$

$$||F(q) - R^T T_y(q)|| \leq K\sqrt{\left(\frac{\left(2^{\frac{u}{2l-1}} - 2^{\frac{u-1}{2l-1}}\right)^{2p+1}}{(2p+1)}\right)}.$$

□

3.1. **Operational matrix of Integration.** Integrate $\xi_{u,v}(q)$ wrt q and represent it as linear combination of Taylor wavelet basis.

$$\int_0^q \xi_{1,0}(q)dq = \left[0 \quad \frac{780}{1351} \quad 0 \quad 0 \quad 0 \quad 0 \quad 0 \quad 0 \quad 0 \quad 0\right] T_{y10}(q),$$

$$\int_0^q \xi_{1,1}(q)dq = \left[0 \quad 0 \quad \frac{744}{1921} \quad 0 \quad 0 \quad 0 \quad 0 \quad 0 \quad 0 \quad 0\right] T_{y10}(q),$$

$$\int_0^q \xi_{1,2}(q)dq = \left[0 \quad 0 \quad 0 \quad \frac{282}{1001} \quad 0 \quad 0 \quad 0 \quad 0 \quad 0 \quad 0\right] T_{y10}(q),$$

$$\int_0^q \xi_{1,3}(q)dq = \left[0 \quad 0 \quad 0 \quad 0 \quad \frac{506}{2295} \quad 0 \quad 0 \quad 0 \quad 0 \quad 0\right] T_{y10}(q),$$

$$\int_0^q \xi_{1,4}(q)dq = \left[0 \quad 0 \quad 0 \quad 0 \quad 0 \quad \frac{415}{2294} \quad 0 \quad 0 \quad 0 \quad 0\right] T_{y10}(q),$$

$$\int_0^q \xi_{1,5}(q)dq = \left[0 \quad 0 \quad 0 \quad 0 \quad 0 \quad 0 \quad \frac{595}{3881} \quad 0 \quad 0 \quad 0\right] T_{y10}(q),$$

$$\int_0^q \xi_{1,6}(q)dq = \left[0 \quad 0 \quad 0 \quad 0 \quad 0 \quad 0 \quad 0 \quad \frac{807}{6068} \quad 0 \quad 0\right] T_{y10}(q),$$

$$\int_0^q \xi_{1,7}(q)dq = \left[0 \quad 0 \quad 0 \quad 0 \quad 0 \quad 0 \quad 0 \quad 0 \quad \frac{1051}{8951} \quad 0\right] T_{y10}(q),$$

$$\int_0^q \xi_{1,8}(q)dq = \left[0 \quad 0 \quad 0 \quad 0 \quad 0 \quad 0 \quad 0 \quad 0 \quad 0 \frac{1327}{12626}\right] T_{y10}(q),$$

$$\int_0^q \xi_{1,9}(q)dq = \left[0 \quad 0 \quad 0 \quad 0 \quad 0 \quad 0 \quad 0 \quad 0 \quad 0 \quad 0\right] T_{y10}(q) + \frac{76}{799}\xi_{1,11}(q),$$

This implies,

$$\int_0^q T_{y10}(q)dq = S_{10\times 10} T_{y10}(q) + \hat{T}_{y10}(q),$$

where

$$S=\begin{bmatrix} 0 & \frac{780}{1351} & 0 & 0 & 0 & 0 & 0 & 0 & 0 & 0 \\ 0 & 0 & \frac{744}{1921} & 0 & 0 & 0 & 0 & 0 & 0 & 0 \\ 0 & 0 & 0 & \frac{282}{1001} & 0 & 0 & 0 & 0 & 0 & 0 \\ 0 & 0 & 0 & 0 & \frac{506}{2295} & 0 & 0 & 0 & 0 & 0 \\ 0 & 0 & 0 & 0 & 0 & \frac{415}{2294} & 0 & 0 & 0 & 0 \\ 0 & 0 & 0 & 0 & 0 & 0 & \frac{595}{3881} & 0 & 0 & 0 \\ 0 & 0 & 0 & 0 & 0 & 0 & 0 & \frac{807}{6068} & 0 & 0 \\ 0 & 0 & 0 & 0 & 0 & 0 & 0 & 0 & \frac{1051}{8951} & 0 \\ 0 & 0 & 0 & 0 & 0 & 0 & 0 & 0 & 0 & \frac{1327}{12626} \end{bmatrix}, \text{ and } \hat{T}_{y10}(q)=\begin{bmatrix} 0 \\ 0 \\ 0 \\ 0 \\ 0 \\ 0 \\ 0 \\ 0 \\ 0 \\ \frac{76}{799}\xi_{1,11}(q) \end{bmatrix},$$

Integrating $\xi_{u,v}(q)$ twice wrt q and representing it as linear combination of Taylor wavelet basis.

$$\int_0^q\int_0^q \xi_{1,0}(q)dqdq = \begin{bmatrix} 0 & 0 & \frac{646}{2889} & 0 & 0 & 0 & 0 & 0 & 0 & 0 \end{bmatrix} T_{y10}(q)(\xi),$$

$$\int_0^q\int_0^q \xi_{1,1}(q)dqdq = \begin{bmatrix} 0 & 0 & 0 & \frac{660}{6049} & 0 & 0 & 0 & 0 & 0 & 0 \end{bmatrix} T_{y10}(q),$$

$$\int_0^q\int_0^q \xi_{1,2}(q)dqdq = \begin{bmatrix} 0 & 0 & 0 & 0 & \frac{321}{5168} & 0 & 0 & 0 & 0 & 0 \end{bmatrix} T_{y10}(q),$$

$$\int_0^q\int_0^q \xi_{1,3}(q)dqdq = \begin{bmatrix} 0 & 0 & 0 & 0 & 0 & \frac{701}{17575} & 0 & 0 & 0 & 0 \end{bmatrix} T_{y10}(q),$$

$$\int_0^q\int_0^q \xi_{1,4}(q)dqdq = \begin{bmatrix} 0 & 0 & 0 & 0 & 0 & 0 & \frac{1297}{46764} & 0 & 0 & 0 \end{bmatrix} T_{y10}(q),$$

$$\int_0^q\int_0^q \xi_{1,5}(q)dqdq = \begin{bmatrix} 0 & 0 & 0 & 0 & 0 & 0 & 0 & \frac{22}{1079} & 0 & 0 \end{bmatrix} T_{y10}(q),$$

$$\int_0^q\int_0^q \xi_{1,6}(q)dqdq = \begin{bmatrix} 0 & 0 & 0 & 0 & 0 & 0 & 0 & 0 & \frac{26}{1665} & 0 \end{bmatrix} T_{y10}(q),$$

$$\int_0^q\int_0^q \xi_{1,7}(q)dqdq = \begin{bmatrix} 0 & 0 & 0 & 0 & 0 & 0 & 0 & 0 & 0 & \frac{30}{2431} \end{bmatrix} T_{y10}(q),$$

$$\int_0^q\int_0^q \xi_{1,8}(q)dqdq = \begin{bmatrix} 0 & 0 & 0 & 0 & 0 & 0 & 0 & 0 & 0 & 0 \end{bmatrix} T_{y10}(q) + \frac{34}{3401}\xi_{1,11}(q),$$

$$\int_0^q\int_0^q \xi_{1,9}(q)dqdq = \begin{bmatrix} 0 & 0 & 0 & 0 & 0 & 0 & 0 & 0 & 0 & 0 \end{bmatrix} T_{y10}(q) + \frac{38}{4599}\xi_{1,12}(q),$$

This implies,

$$\int_0^q\int_0^q T_{y10}(q)dqdq = S'_{10\times 10}T_{y10}(q) + \hat{T}'_{y10}(q),$$

where

$$S' = \begin{bmatrix} 0 & 0 & \frac{646}{2889} & 0 & 0 & 0 & 0 & 0 & 0 & 0 \\ 0 & 0 & 0 & \frac{660}{6049} & 0 & 0 & 0 & 0 & 0 & 0 \\ 0 & 0 & 0 & 0 & \frac{321}{5168} & 0 & 0 & 0 & 0 & 0 \\ 0 & 0 & 0 & 0 & 0 & \frac{701}{17575} & 0 & 0 & 0 & 0 \\ 0 & 0 & 0 & 0 & 0 & 0 & \frac{1297}{46764} & 0 & 0 & 0 \\ 0 & 0 & 0 & 0 & 0 & 0 & 0 & \frac{22}{1079} & 0 & 0 \\ 0 & 0 & 0 & 0 & 0 & 0 & 0 & 0 & \frac{26}{1665} & 0 \\ 0 & 0 & 0 & 0 & 0 & 0 & 0 & 0 & 0 & \frac{30}{2431} \\ 0 & 0 & 0 & 0 & 0 & 0 & 0 & 0 & 0 & 0 \\ 0 & 0 & 0 & 0 & 0 & 0 & 0 & 0 & 0 & 0 \end{bmatrix} \text{ and } \hat{T}'_{y10}(q) = \begin{bmatrix} 0 \\ 0 \\ 0 \\ 0 \\ 0 \\ 0 \\ 0 \\ 0 \\ 0 \\ \frac{34}{3401}\xi_{1,11}(q) \\ \frac{38}{4599}\xi_{1,12}(q) \end{bmatrix},$$

Integrating $\xi_{u,v}(q)$ thrice wrt q between and representing it as linear combination of Taylor wavelet basis.

$$\int_0^q \int_0^q \int_0^q \xi_{1,0}(q)dqdqdq = \begin{bmatrix} 0 & 0 & 0 & \frac{255}{4048} & 0 & 0 & 0 & 0 & 0 & 0 \end{bmatrix} T_{y10}(q),$$

$$\int_0^q \int_0^q \int_0^q \xi_{1,1}(q)dqdqdq = \begin{bmatrix} 0 & 0 & 0 & 0 & \frac{65}{2702} & 0 & 0 & 0 & 0 & 0 \end{bmatrix} T_{y10}(q),$$

$$\int_0^q \int_0^q \int_0^q \xi_{1,2}(q)dqdqdq = \begin{bmatrix} 0 & 0 & 0 & 0 & 0 & \frac{175}{15841} & 0 & 0 & 0 & 0 \end{bmatrix} T_{y10}(q),$$

$$\int_0^q \int_0^q \int_0^q \xi_{1,3}(q)dqdqdq = \begin{bmatrix} 0 & 0 & 0 & 0 & 0 & 0 & \frac{77}{12592} & 0 & 0 & 0 \end{bmatrix} T_{y10}(q),$$

$$\int_0^q \int_0^q \int_0^q \xi_{1,4}(q)dqdqdq = \begin{bmatrix} 0 & 0 & 0 & 0 & 0 & 0 & 0 & \frac{46}{12471} & 0 & 0 \end{bmatrix} T_{y10}(q),$$

$$\int_0^q \int_0^q \int_0^q \xi_{1,5}(q)dqdqdq = \begin{bmatrix} 0 & 0 & 0 & 0 & 0 & 0 & 0 & 0 & \frac{37}{15455} & 0 \end{bmatrix} T_{y10}(q),$$

$$\int_0^q \int_0^q \int_0^q \xi_{1,6}(q)dqdqdq = \begin{bmatrix} 0 & 0 & 0 & 0 & 0 & 0 & 0 & 0 & 0 & \frac{49}{29856} \end{bmatrix} T_{y10}(q),$$

$$\int_0^q \int_0^q \int_0^q \xi_{1,7}(q)dqdqdq = \begin{bmatrix} 0 & 0 & 0 & 0 & 0 & 0 & 0 & 0 & 0 & 0 \end{bmatrix} T_{y10}(q) + \frac{17}{60486}\xi_{1,11}(q),$$

$$\int_0^q \int_0^q \int_0^q \xi_{1,8}(q)dqdqdq = \begin{bmatrix} 0 & 0 & 0 & 0 & 0 & 0 & 0 & 0 & 0 & 0 \end{bmatrix} T_{y10}(q) + \frac{17}{19576}\xi_{1,12}(q),$$

$$\int_0^q \int_0^q \int_0^q \xi_{1,9}(q)dqdqdq = \begin{bmatrix} 0 & 0 & 0 & 0 & 0 & 0 & 0 & 0 & 0 & 0 \end{bmatrix} T_{y10}(q) + \frac{7}{10599}\xi_{1,13}(q),$$

This implies,

$$\int_0^q \int_0^q \int_0^q T_{y10}(q)dqdqdq = S''_{10\times 10}T_{y10}(q) + \hat{T}''_{y10}(q),$$

where

$$S'' = \begin{bmatrix} 0 & 0 & 0 & \frac{255}{4048} & 0 & 0 & 0 & 0 & 0 & 0 \\ 0 & 0 & 0 & 0 & \frac{65}{2702} & 0 & 0 & 0 & 0 & 0 \\ 0 & 0 & 0 & 0 & 0 & \frac{175}{15841} & 0 & 0 & 0 & 0 \\ 0 & 0 & 0 & 0 & 0 & 0 & \frac{77}{12592} & 0 & 0 & 0 \\ 0 & 0 & 0 & 0 & 0 & 0 & 0 & \frac{46}{12471} & 0 & 0 \\ 0 & 0 & 0 & 0 & 0 & 0 & 0 & 0 & \frac{37}{15455} & 0 \\ 0 & 0 & 0 & 0 & 0 & 0 & 0 & 0 & 0 & \frac{49}{29856} \\ 0 & 0 & 0 & 0 & 0 & 0 & 0 & 0 & 0 & 0 \\ 0 & 0 & 0 & 0 & 0 & 0 & 0 & 0 & 0 & 0 \\ 0 & 0 & 0 & 0 & 0 & 0 & 0 & 0 & 0 & 0 \end{bmatrix}, \text{ and } \hat{T}''_{y10}(q) = \begin{bmatrix} 0 \\ 0 \\ 0 \\ 0 \\ 0 \\ 0 \\ \frac{17}{60486}\xi_{1,11}(q) \\ \frac{17}{195576}\xi_{1,12}(q) \\ \frac{7}{10599}\xi_{1,13}(q) \end{bmatrix},$$

Integrating $\xi_{u,v}(q)$ fourth time wrt q and representing it as linear combination of Taylor wavelet basis.

$$\int_0^q\int_0^q\int_0^q\int_0^q \xi_{1,0}(q)dqdqdqdq = \begin{bmatrix} 0 & 0 & 0 & 0 & \frac{1}{72} & 0 & 0 & 0 & 0 & 0 \end{bmatrix} T_{y10}(q),$$

$$\int_0^q\int_0^q\int_0^q\int_0^q \xi_{1,1}(q)dqdqdqdq = \begin{bmatrix} 0 & 0 & 0 & 0 & 0 & \frac{23}{5285} & 0 & 0 & 0 & 0 \end{bmatrix} T_{y10}(q),$$

$$\int_0^q\int_0^q\int_0^q\int_0^q \xi_{1,2}(q)dqdqdqdq = \begin{bmatrix} 0 & 0 & 0 & 0 & 0 & 0 & \frac{29}{16834} & 0 & 0 & 0 \end{bmatrix} T_{y10}(q),$$

$$\int_0^q\int_0^q\int_0^q\int_0^q \xi_{1,3}(q)dqdqdqdq = \begin{bmatrix} 0 & 0 & 0 & 0 & 0 & 0 & 0 & \frac{41}{50415} & 0 & 0 \end{bmatrix} T_{y10}(q),$$

$$\int_0^q\int_0^q\int_0^q\int_0^q \xi_{1,4}(q)dqdqdqdq = \begin{bmatrix} 0 & 0 & 0 & 0 & 0 & 0 & 0 & 0 & \frac{16}{36943} & 0 \end{bmatrix} T_{y10}(q),$$

$$\int_0^q\int_0^q\int_0^q\int_0^q \xi_{1,5}(q)dqdqdqdq = \begin{bmatrix} 0 & 0 & 0 & 0 & 0 & 0 & 0 & 0 & 0 & \frac{19}{75512} \end{bmatrix} T_{y10}(q),$$

$$\int_0^q\int_0^q\int_0^q\int_0^q \xi_{1,6}(q)dqdqdqdq = \begin{bmatrix} 0 & 0 & 0 & 0 & 0 & 0 & 0 & 0 & 0 & 0 \end{bmatrix} T_{y10}(q) + \frac{11}{70463}\xi_{1,11}(q),$$

$$q\int_0^q\int_0^q\int_0^q\int_0^q \xi_{1,7}(\xi)dqdqdqdq = \begin{bmatrix} 0 & 0 & 0 & 0 & 0 & 0 & 0 & 0 & 0 & 0 \end{bmatrix} T_{y10}(q) + \frac{6}{58843}\xi_{1,12}(q),$$

$$\int_0^q\int_0^q\int_0^q\int_0^q \xi_{1,8}(q)dqdqdqdq = \begin{bmatrix} 0 & 0 & 0 & 0 & 0 & 0 & 0 & 0 & 0 & 0 \end{bmatrix} T_{y10}(q) + \frac{8}{115253}\xi_{1,13}(q),$$

$$\int_0^q\int_0^q\int_0^q\int_0^q \xi_{1,9}(q)dqdqdqdq = \begin{bmatrix} 0 & 0 & 0 & 0 & 0 & 0 & 0 & 0 & 0 & 0 \end{bmatrix} T_{y10}(q) + \frac{13}{265929}\xi_{1,14}(q),$$

This implies,

$$\int_0^q\int_0^q\int_0^q\int_0^q T_{y10}(q)dqdqdqdq = S'''_{10\times 10}T_{y10}(q) + \hat{T}'''_{y10}(q),$$

where

$$S''' = \begin{bmatrix} 0 & 0 & 0 & 0 & \frac{1}{72} & 0 & 0 & 0 & 0 & 0 \\ 0 & 0 & 0 & 0 & 0 & \frac{23}{5285} & 0 & 0 & 0 & 0 \\ 0 & 0 & 0 & 0 & 0 & 0 & \frac{29}{16834} & 0 & 0 & 0 \\ 0 & 0 & 0 & 0 & 0 & 0 & 0 & \frac{41}{50415} & 0 & 0 \\ 0 & 0 & 0 & 0 & 0 & 0 & 0 & 0 & \frac{16}{36943} & 0 \\ 0 & 0 & 0 & 0 & 0 & 0 & 0 & 0 & 0 & \frac{19}{75512} \\ 0 & 0 & 0 & 0 & 0 & 0 & 0 & 0 & 0 & 0 \\ 0 & 0 & 0 & 0 & 0 & 0 & 0 & 0 & 0 & 0 \\ 0 & 0 & 0 & 0 & 0 & 0 & 0 & 0 & 0 & 0 \\ 0 & 0 & 0 & 0 & 0 & 0 & 0 & 0 & 0 & 0 \end{bmatrix}, \text{ and } \hat{T}'''_{y10}(q) = \begin{bmatrix} 0 \\ 0 \\ 0 \\ 0 \\ 0 \\ \frac{11}{70463}\xi_{1,11}(q) \\ \frac{6}{58843}\xi_{1,12}(q) \\ \frac{8}{115253}\xi_{1,13}(q) \\ \frac{13}{265929}\xi_{1,14}(q) \end{bmatrix},$$

Similarly, on repeated integration we get higher order Operational integration matrix.

4. Method of solution

In order to convert semi-infinte interval $[0, \infty)$ to finite interval [0,1] we make use of the transformtion $\delta = \frac{\eta}{\eta_\infty}$ and $F(\delta) = \frac{f(\eta)}{\eta_\infty}$,

$$\eta_\infty^2\left(F'^2 - FF'' - 2\gamma F''^2 + \left(Msin^2(\tau) + Da^{-1}\right)F'\right) - F''' - \beta\left(2F'F''' - FF'''' + 3F''^2\right) = 0, \tag{4.1}$$

corresponding boundary constraints are

$$F(0) = 0,\ F'(0) = 1,\ F'(1) = 0,\ \text{and } F''(1) = 0. \tag{4.2}$$

Let us assume that

$$F''''(\delta) = G^T T_{y10}(\delta), \tag{4.3}$$

where $G^T = [g_1,\ g_2,\ g_3,\ g_4,\ g_5,\ g_6,\ g_7,\ g_8,\ g_9,\ g_{10}]$.
Integrating Eq. (4.3) wrt δ

$$F'''(\delta) = F'''(0) + G^T[\hat{T}_{y10}(\delta) + ST_{y10}(\delta)], \tag{4.4}$$

Integrating Eq. (4.4) wrt δ

$$F''(\delta) = F''(0) + \delta F'''(0) + G^T[\hat{T}_{y10}(\delta) + S'T_{y10}(\delta)], \tag{4.5}$$

Integrating Eq. (4.5) wrt δ and substituting $F'(0) = 1$ we get

$$F'(\delta) = 1 + \delta F''(0) + \frac{\delta^2}{2}F'''(0) + G^T[\hat{T}''_{y10}(\delta) + S''T_{y10}(\delta)], \tag{4.6}$$

Integrating Eq. (4.6) wrt δ and substituting $F(0) = 0$

$$F(\delta) = \delta + \frac{\delta^2}{2}F''(0) + \frac{\delta^3}{6}F'''(0) + G^T[\hat{T}'''_{y10}(\delta) + S'''T_{y10}(\delta)], \tag{4.7}$$

Substituting $\delta = 1$ in Eqs. (4.5) and (4.6) we get

$$F''(1) = F''(0) + F'''(0) + G^T[\hat{T}'_{y10}(\delta) + S'T_{y10}(\delta)]\big|_{\delta=1}, \tag{4.8}$$

$$0 = F''(0) + F'''(0) + G^T[\hat{T}'_{y10}(\delta) + S'T_{y10}(\delta)]\big|_{\delta=1}, \tag{4.9}$$

$$F'(1) = 1 + F''(0) + \frac{1}{2}F'''(0) + G^T[\hat{T}''_{y10}(\delta) + S''T_{y10}(\delta)]\big|_{\delta=1},$$

$$0 = 1 + F''(0) + \frac{1}{2}F'''(0) + G^T[\hat{T}''_{y10}(\delta) + S''T_{y10}(\delta)]\big|_{\delta=1}, \tag{4.10}$$

solving Eqs. (4.9) and (4.10) we get

$$F'''(0) = 2\left[1 + G^T[\hat{T}^{''}_{y10}(\delta) + S''T_{y10}(\delta)]\big|_{\delta=1} - G^T[\hat{T}^{'}_{y10}(\delta) + S'T_{y10}(\delta)]\big|_{\delta=1}\right], \tag{4.11}$$

$$F''(0) = -\left[2\left[1 + G^T[\hat{T}^{''}_{y10}(\delta) + S''T_{y10}(\delta)]\big|_{\delta=1} - G^T[\hat{T}^{'}_{y10}(\delta) + S'T_{y10}(\delta)]\big|_{\delta=1}\right] + G^T[\hat{T}^{'}_{y10}(\delta) + S'V(\delta)]\big|_{\delta=1}\right], \tag{4.12}$$

Now substituting $F(\delta)$, $F'(\delta)$, $F''(\delta)$, $F'''(\delta)$and $F''''(\delta)$ into the momentum equation we get system of non linear equations. The unkown coefficients are found by using the collocating points $\delta_i = \frac{2i-1}{2N}$ where $i = 1, 2, 3, ...$

Substitute the obtained coefficient values in Eq. (4.3) to Eq. (4.8) to get numerial solutions to Eqs. (4.1) and (4.2). By substituting the transformation we get numerical solution to Eqs. (2.11) and (2.12).

The local skinfriction is given by

$$\begin{aligned} F''(0) &= -(1-3\beta)\left[2\left[1 + G^T[\hat{T}^{''}_{y10}(\delta) + S''T_{y10}(\delta)]\big|_{\delta=1} - G^T[\hat{T}^{'}_{y10}(\delta) + S'T_{y10}(\delta)]\big|_{\delta=1}\right]\right. \\ &+ \left. G^T[\hat{T}^{'}_{y10}(\delta) + S'T_{y10}(\delta)]\big|_{\delta=1}\right], \end{aligned} \tag{4.13}$$

substituting $F''(0) = \delta_\infty f''(0)$

$$\begin{aligned} f''(0) &= -\frac{1-3\beta}{\delta_\infty}\left[2\left[1 + G^T[\hat{T}^{''}_{y10}(\delta) + S''T_{y10}(\delta)]\big|_{\delta=1} - G^T[\hat{T}^{'}_{y10}(\delta) + S'T_{y10}(\delta)]\big|_{\delta=1}\right]\right. \\ &+ \left. G^T[\hat{T}^{'}_{y10}(\delta) + S'T_{y10}(\delta)]\big|_{\delta=1}\right]. \end{aligned} \tag{4.14}$$

5. Numerical Implementation

$F'''(\delta), F''(\delta), F'(\delta)$ and $F(\delta)$ using Taylor Wavelet method at $V = 10$ is investigated numerically for MHD Rivlin Ericksen fluid flow. The parameters that are fixed : $\beta = 0.4, \gamma = 0.2, M = 5, \tau = \pi/4, Da^{-1} = 5$. We get the unknown coefficients as follows:

$g_1 = \frac{36737}{94}$, $g_2 = \frac{-66876}{5}$, $g_3 = \frac{320063}{3}$, $g_4 = -423616$, $g_5 = 960579$,
$g_6 = -1246922$, $g_7 = 787999$, $g_8 = \frac{-4639}{130}$, $g_9 = -284194$, $g_{10} = 112613$.

On substituting these unknown values in Eq. (4.3) to Eq. (4.8) we get $F''''(\delta), F'''(\delta), F''(\delta), F'(\delta)$ and $F(\delta)$. From the obtained $F''''(\delta), F'''(\delta), F''(\delta), F'(\delta)$ and F and the cordinate transformations we obtain $f''''(\eta), f''(\eta)', f''(\eta), f'(\eta)$ and $f(\eta)$.

$$\begin{aligned} F'(\delta) &= \frac{3941455\delta^{12}}{10599} - \frac{2415649\sqrt{23}\delta^{11}}{9788} - \frac{4639\sqrt{21}\delta^{10}}{462540} + \frac{38611951\sqrt{19}\delta^{9}}{29856} \\ &- \frac{46136114\sqrt{17}\delta^{8}}{15455} + \frac{14728878\sqrt{15}\delta^{7}}{4157} - \frac{2038652\sqrt{13}\delta^{6}}{787} \\ &+ \frac{652505335849112947\sqrt{11}\delta^{5}}{544292615487488} - \frac{1304082\delta^{4}}{1351} + \frac{9367935\sqrt{7}\delta^{3}}{380512} \\ &+ \frac{41882838958306\delta^{2}}{450359962737049} - \frac{77226166866220\delta}{4503599627370496} + 1, \end{aligned} \tag{5.1}$$

TABLE 1. comparison of Skin friction coefficient by Taylor wavelet method with bvp4c for $\tau = \pi/4$, $Da^{-1} = 5$.

M	β	γ	-(1-3β)f"(0) by Taylor wavelet method	-(1-3β)f"(0) by bvp4c
1	1	1	-1.97892200	-1.97838391
2	1	1	-2.05319515	-2.05278039
2	2	1	-4.06853807	-4.06433668
2	2	2	-3.73329571	-3.73633766

TABLE 2. comparison of f"(0) by Taylor wavelet method with exact solution for β=γ =0.

M	τ	Da^{-1}	f"(0) by Taylor wavelet method	f"(0) by exact solution
0	0	0	-0.9999353093	-1
1	$\pi/2$	1	-1.73206586515	-1.7320508075
2	$\pi/3$	2	-2.12154605898	-2.1213203435
3	$\pi/4$	3	-2.34506229156	-2.3452078799

TABLE 3. comparison of f"(0) by Taylor wavelet method with Akbar *et.al* [1] for β=γ=Da^{-1}=0 and $\tau = \pi/2$.

M	f"(0) by Taylor wavelet method	f"(0) by Akbar *et.al* [1]
0	-0.9999353093	-1
1	-1.4148832238	-1.41421
5	-2.44918240569	-2.44949
10	-3.31697827	-3.31663

$$
\begin{aligned}
F(\delta) \;=\; & \frac{12186167649941675602 47\sqrt{3}\delta^{13}}{737869762948382064 64} - \frac{22743243062149410029 5\delta^{12}}{2305843009213693952} \\
& - \frac{13917\sqrt{23}\delta^{11}}{3824795} + \frac{8667989\sqrt{21}\delta^{10}}{70463} - \frac{11845759\sqrt{19}\delta^{9}}{37756} + \frac{15369264\sqrt{17}\delta^{8}}{36943} \\
& - \frac{17368256\sqrt{15}\delta^{7}}{50415} + \frac{21261409819802556 7\sqrt{13}\delta^{6}}{1156823671373824} - \frac{1538148\sqrt{11}\delta^{5}}{26425} + \frac{36737\delta^{4}}{2256} \\
& + \frac{418828389583064 9\delta^{3}}{135107988821114 88} - \frac{772261668662203 7\delta^{2}}{9007199254740992} + \delta. \qquad (5.2)
\end{aligned}
$$

Result validation : In the present study we apply taylor wavelet collocation method to obtain solution for differential equation Eq. (2.7) and compare the solution obtained with the bvp4c in Table 1, thus validating the results so obatined. Results are expressed in the form of graphs for various parameters at $\beta = 0.4$, $\gamma = 0.2$, $M = 5$, $Da^{-1} = 5$, $\tau = \pi/4$. Axial velocity and transverse $f_\eta(\eta)$ and $f(\eta)$ is achieved by substituting the coordinate transformation $\delta = \frac{\eta}{\eta_\infty}$ in Eqs. (5.1) and (5.2). With the help of Taylor wavelet operational matrix we obtain the local skin friction and is compared with bvp4c that can be visualized through the Table 1.

6. EXACT SOLUTION

We obtain exact solution for $\beta = \gamma = 0$, equation reduces to

$$f''' + ff'' - f'^2 - (Msin^2(\tau) + Da^{-1})f' = 0, \qquad (6.1)$$

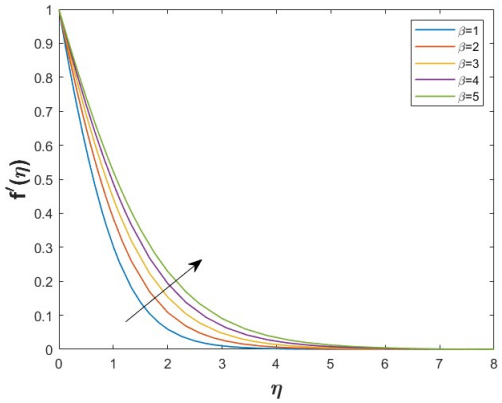

FIGURE 2. Variation of axial velocity for different values of β.

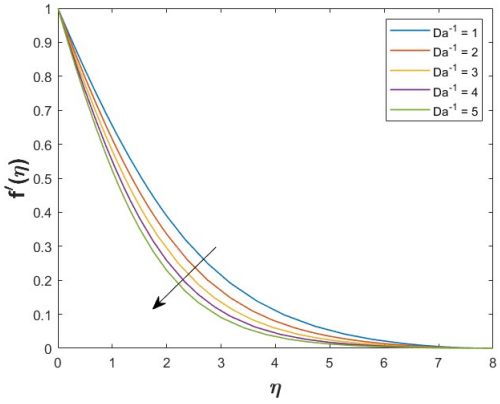

FIGURE 3. Variation of axial velocity for different values of inverse darcy number.

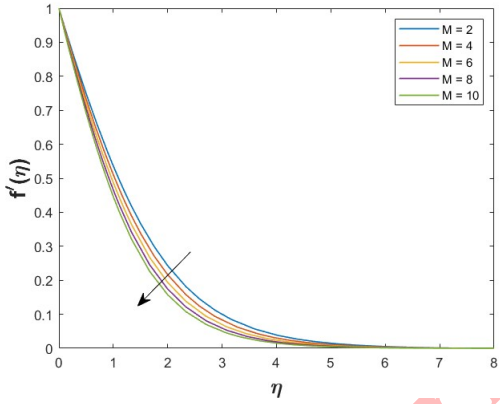

FIGURE 4. Variation of axial velocity for different values of magnetic parameter.

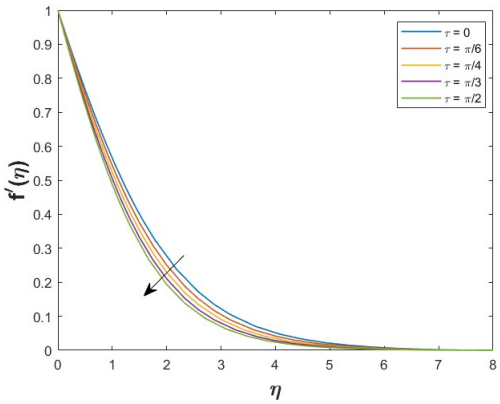

FIGURE 5. Variation of axial velocity for different values of angle of inclination.

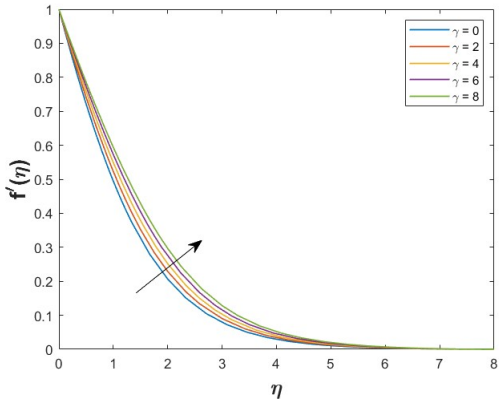

FIGURE 6. Variation of axial velocity for different values of γ.

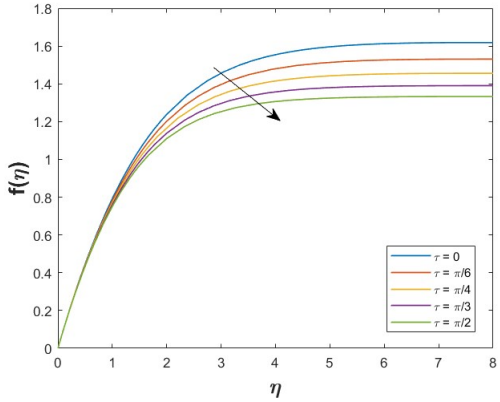

FIGURE 7. Variation of tansverse velocity for different values of angle of inclination.

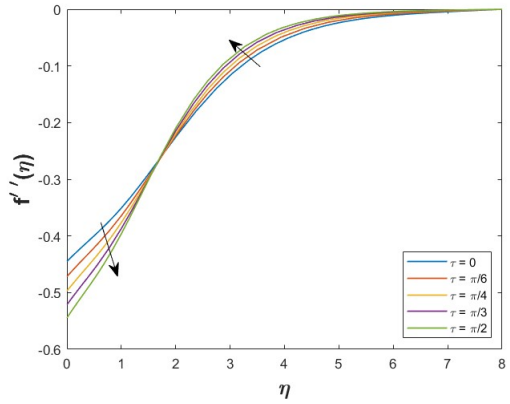

FIGURE 8. Variation of velocity gradient for different values of angle of inclination.

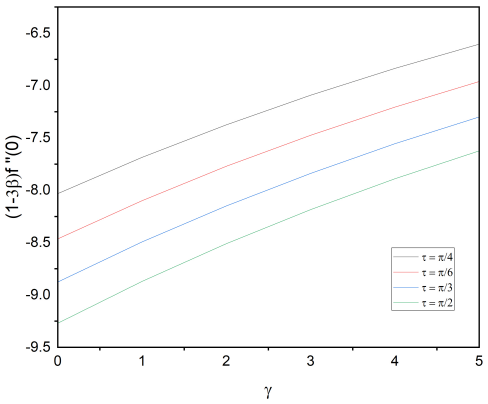

FIGURE 9. Variation of skin friction wrt γ for different values of τ.

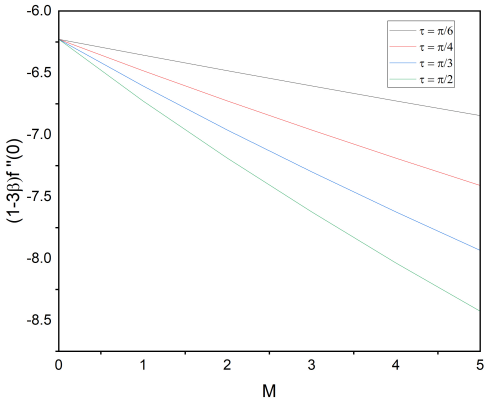

FIGURE 10. Variation of skin friction wrt M for different values of τ.

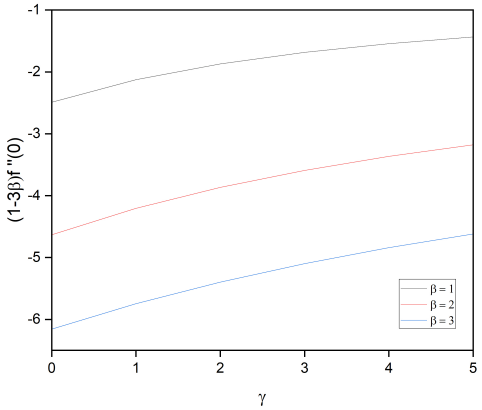

FIGURE 11. Variation of skin friction wrt γ for different values of β.

subject to boundary conditions

$$f(0) = 0, \quad f'(0) = 1 \quad and \quad f'(\infty) \to 0, \tag{6.2}$$

we obtain solution as

$$f(\eta) = \frac{1 - \exp^{-\eta\sqrt{Msin^2\tau + Da^{-1}+1}}}{\sqrt{Msin^2\tau + Da^{-1}+1}}. \tag{6.3}$$

$$Thus \quad f''(0) = -\sqrt{Msin^2\tau + Da^{-1}+1}. \tag{6.4}$$

7. Results and Discussions

It can be observed that axial velocity decreases along η due to decline of friction from the stretching surface. From Figure 2 it is clear that increased viscoelastic parameter increases the axial velocity due to the elastic property of the

fluid. Increase in inverse darcy number decreases the axial velocity due to the porosity of the stretching sheet as seen in Figure 3.

From Figure 4 it can be observed that increase in magnetic field leads to decrease in axial velocity because magnetic field retards the fluid flow making fluid to flow slowly. Orientation of magnetic field also plays a vital role in controlling the fluid flow, from Figure 5 it could be observed that as inclination of magnetic filed is increased from 0 to $\pi/2$ axial velocity decreases.

Increase in cross viscous parameter increases the axial velocity as seen in Figure 6.

The effect of angle of inclination on transverse velocity is depicted in Figure 7, it could be concluded that increase in τ decreases the transverse velocity.

From Figure 8 it is clear that the distribution of velocity gradient decreases for increase in angle of inclination within the boundary layer, further which increase in angle of inclination increases the distribution of velocity gradient.

The influence of various parameters on local skin friction coefficient is depicted in Figures 9-11. In Figure 9 variation of local skin friction coefficient wrt γ for various values of τ is studied, it is clear that increase in τ numerically increases the local skin friction . In Figure 10 variation of local skin friction coefficient wrt M for various values of τ is depicted, it could be noted that increase in τ numerically increases the local skin friction coefficient, further in Figure 11 variation of local skin friction coefficient wrt γ is studied for various values of β and it could be infered that increase in β numerically increases the local skin friction coefficient.

In Table 1 comaparison of local skin friction coeffecient for various values of M, β and γ with bvp4c is done. It could be infered that local skin friction coeffecient values by taylor wavelet method have a clear agrement with bvp4c with very less error.

8. Conclusion

The Taylor wavelet operational matrix approach has been developed to investigate Revlin Ericksen fluid moving across a stretching sheet in the vicinity of a magnetic field. The mentioned computational method is utilized to handle boundary valued nonliner ordinary differential equation and solution obtained via this method has a clear agreement with the values obtaiend via bvp4c with very less error in the solution. The results of the present investigation are presented in an assortment of graphs and tables.

- Axial velocity propels with a raise in the cross viscous parameter and viscoelastic parameter.
- The axial velocity drops as the inverse darcy number, magnetic field, and inclination angle grows.
- Table 1 and the Figures show the way local skin friction alters with different parameters.

References

[1] N. S. Akbar , A. Ebaid and Z. H. Khan, *Numerical analysis of magnetic field effects on Eyring-Powell fluid flow towards a stretching sheet*, Journal of magnetism and Magnetic Materials, *382*, 355-358.

[2] R. Chand and G. C. Rana, *Thermal Instability of Rivlin–Ericksen elastico-viscous nanofluid saturated by a porous medium*, Journal of fluids engineering, *134*(12) (2012), 121203.

[3] L. J. Crane, *Flow past a stretching plate*, Z. Angew Math. Phys., *21* (1970), 645.

[4] N. Dalir, *Numerical study of entropy generation for forced convection flow and heat transfer of a Jeffrey fluid over a stretching sheet*, Alexandria Engineering Journal, *53*(4) (2014), 769-778.

[5] D. Dharamendra, M. K. Awasthi, V. Kumar, A. Chauhan, and N. Dhiman, *Study of instability of Rivlin-Ericksen viscoelastic fluid film*, AIP Conference Proceedings, AIP Publishing. *2481*(1) (2022).

[6] S. Gümgüm, *Taylor wavelet solution of linear and nonlinear Lane-Emden equations*, Applied Numerical Mathematics, *158* (2020), 44-53.

[7] U. Gupta, P. Aggarwal, and K. R. Wanchoo, *Thermal convection of dusty compressible Rivlin-Ericksen viscoelastic fluid with Hall currents*, Thermal Science, *16*(1) (2012), 177-192.

[8] P. M. Jordan and P. Puri, *Stokes' first problem for a Rivlin–Ericksen fluid of second grade in a porous half-space*, International Journal of Non-Linear Mechanics, *38*(7) (2003), 1019-1025.

[9] R. A. Kareem, S. O. Salawu, and Y. Yan, *Analysis of transient Rivlin-Ericksen fluid and irreversibility of exothermic reactive hydromagnetic variable viscosity*, J. Appl. Comput. Mech., *6*(1) (2020), 26-36.

[10] E. Keshavarz, Y. Ordokhani, and M. Razzaghi, *The Taylor wavelets method for solving the initial and boundary value problems of Bratu-type equations*, Applied Numerical Mathematics, *128* (2018), 205-216.
[11] P. Kumar, H. Mohan, and R. Lal, *Effect of magnetic field on thermal instability of a rotating Rivlin-Ericksen viscoelastic fluid*, Int. J. Math. Math. Sci., *2006*(3) (2006), 1-10.
[12] P. A. Kumar and G. J. Singh, *Stability of two superposed Rivlin-Ericksen viscoelastic fluids in the presence of suspended particles*, Romanian Journal of Physics, *51*(9) (2006), 927.
[13] S. Kumbinarasaiah and K. R. Raghunatha, *The applications of Hermite wavelet method to nonlinear differential equations arising in heat transfer*, International Journal of Thermofluids, *9* (2021), 100066.
[14] G. Manohara and S. Kumbinarasaiah, *An innovative Fibonacci wavelet collocation method for the numerical approximation of Emden-Fowler equations*, Applied Numerical Mathematics, (2024).
[15] G. M. Moatimid and A. Sayed, *Nonlinear EHD stability of a cylindrical interface separating two Rivlin-Ericksen fluids: A novel analysis*, Chinese Journal of Physics, *87* (2024), 379-397.
[16] V. Ramareddy, P. M. Basawaraj and U. S. Mahabaleshwar, and B. Souayeh, *An MHD boundary layer flow of Casson fluid due to a moving wedge analyzed by the Bernoulli wavelet method*, ZAMM-Journal of Applied Mathematics and Mechanics/Zeitschrift für Angewandte Mathematik und Mechanik, (2024), e202300648.
[17] B. V. Rathish Kumar and M. Mehra, *Wavelet-Taylor Galerkin method for the Burgers equation*, BIT Numerical Mathematics, *45* (2005), 543-560.
[18] P. C. Reddy , M. C. Raju, G. S. S. Raju, and C. M. Reddy, *Diffusion thermo and thermal diffusion effects on MHD free convection flow of Rivlin-Ericksen fluid past a semi infinite vertical plate*, Bulletin of Pure and Applied Sciences-Mathematics and Statistics, *36*(2) (2017), 266-284.
[19] R. S. Rivlin and J. L. Ericksen, *Stress-deformation relations for isotropic materials*. Collected Papers of RS Rivlin, *Vol* I and II, (1997), 911-1013.
[20] M. N. Sadiq, M. Sajid, T. Javed, and N. Ali, *A numerical study for heat and fluid flow of couple stress fluid over a spiraling disk by Legendre wavelet spectral collocation method*, ZAMM-Journal of Applied Mathematics and Mechanics/Zeitschrift für Angewandte Mathematik und Mechanik, *100*(8) (2020), e201900220.
[21] R. C. Sharma and P. Kumar , *Effect of rotation on thermal instability in Rivlin-Ericksen elastico-viscous fluid*, Zeitschrift für Naturforschung, *51*(7) (1996), 821-824.
[22] V. Sharma , K. Kishor, and Rana G, *The instability of streaming Rivlin-Ericksen fluids in porous medium*, Studia Geotechnica et Mechanica, *23*(3-4) (2001), 83-93.
[23] S. C. Shiralashetti and S. I. Hanaji, *Taylor wavelet collocation method for Benjamin–Bona–Mahony partial differential equations*, Results in Applied Mathematics, *9* (2021), 100139.
[24] A. K. Shukla and M. K. Awasthi, *Stability characteristics of planar Rivlin–Ericksen fluid interface with mass and heat transfer*, Journal of Fluids Engineering, *145*(3) (2023), 031302.
[25] B. Siddappa and P. S. Hiremath, *Rivlin-Ericksen fluid flow past a stretching plate with suction*, Kyungpook Mathematical Journal, *20*(2) (1980), 267-272.
[26] B. Siddappa and B.S. Khapate, *Rivlin–Ericksen fluid flow past a stretching plate*, Rev. Roum. Sci. Techn. -Mec. Appl, *21* (1976), 497–505.
[27] M. Slemrod, *Constitutive Relations for Rivlin-Ericksen Fluids Based on Generalized Rational Approximation*, Archive for rational mechanics and analysis, *146*(1) (1999), 73-93.
[28] P. T. Toan, T. N. Vo, and M. Razzaghi, *Taylor wavelet method for fractional delay differential equations*, Engineering with Computers, *37*(1) (2021), 231-240.
[29] R. Vidya Shree, B. Patil Mallikarjun, and A. J. Chamkha, *Analysis of MHD boundary layer flow of a viscous fluid past a stretching sheet employing the Legendre wavelet method*, International Journal of Ambient Energy, *45*(1) (2024), 2310629.
[30] R. Vidya shree, B. Patil Mallikarjun, and S. Kumbinarasaiah, *Entropy generation on an MHD Casson fluid flow in an inclined channel with a permeable walls through Hermite wavelet method*, Results in Control and Optimization, *12* (2023), 100261.
[31] R. Vidya Shree , B. Patil Mallikarjun and S. Kumbinarasaiah, *Time-varying stretching velocity analysis for an unsteady flow of Williamson fluid by Hermite wavelet*, Journal of Umm Al-Qura University for Applied Sciences,

(2024), 1-14.

[32] A. B. Vishalakshi, U. S. Mahabaleshwar, and Y. Sheikhnejad, *Impact of MHD and mass transpiration on Rivlin–Ericksen liquid flow over a stretching sheet in a porous media with thermal communication*, Transport in Porous Media, *142*(1) (2022), 353-381.

[33] Vivek and M. Kumar, *Bernoulli wavelet application to the numerical solution of Jeffery–Hamel flow problem*, Numerical Heat Transfer, Part B: Fundamentals, (2024), 1-20.